

# Tunneling evidence of half-metallicity in epitaxial films of ferromagnetic perovskite manganites and ferrimagnetic magnetite

J. Y. T. Wei<sup>a)</sup> and N.-C. Yeh

*Department of Physics, California Institute of Technology, Pasadena, California 91125*

R. P. Vasquez

*Center for Space Microelectronics Technology, Jet Propulsion Laboratory, California Institute of Technology, Pasadena, California 91109*

A. Gupta

*IBM, Thomas J. Watson Research Center, Yorktown Heights, New York 10598*

Direct evidence of half-metallic density of states is observed by scanning tunneling spectroscopy of ferromagnetic  $\text{La}_{0.7}\text{Ca}_{0.3}\text{MnO}_3$  and  $\text{La}_{1-x}\text{Sr}_x\text{MnO}_3$  ( $x=0.3, 0.33$ ) epitaxial films which exhibit colossal magnetoresistance (CMR). At 77 K, well below the Curie temperatures, the normalized tunneling conductance  $(dI/dV)/\langle I/V \rangle$  for all samples exhibits similar pronounced peak structures, consistent with the spin-split density of states spectra for the itinerant bands in the ferromagnetic state. The exchange energy splitting between the majority and minority spins, as well as an apparent energy gap near the Fermi level, show variations with the chemical composition and the temperature. For comparison, the tunneling spectrum of a half-metallic ferrimagnet  $\text{Fe}_3\text{O}_4$  is also studied. The characteristic spin-split density of states spectrum is observed, and the similarities and differences of  $\text{Fe}_3\text{O}_4$  compared with the perovskite manganites are discussed. © 1998 American Institute of Physics. [S0021-8979(98)45811-0]

Half-metallic ferromagnetic materials, characterized by the presence of an energy gap for one of the spin orientations at the Fermi level and continuous bands for the other, have been a subject of interest for more than a decade.<sup>1-4</sup> An important consequence of the half-metallicity is the complete spin polarization in the ferromagnetic state of these materials,<sup>1,2</sup> giving rise to novel physical properties, such as very large magneto-optical Kerr effects<sup>5</sup> in the Heusler alloys (e.g., PtMnSb).<sup>6</sup> Recently, the intensively studied phenomenon of negative colossal magnetoresistance (CMR) in the perovskite manganites,  $\text{Ln}_{1-x}\text{M}_x\text{MnO}_3$  (Ln: trivalent rare earth ions, M=divalent alkaline earth ions), has been attributed to the half-metallic characteristics of these materials based on electronic band structure calculations<sup>7</sup> and on various supportive though indirect experiments.<sup>8,9</sup> In this work, we provide temperature-dependent tunneling spectroscopy data as direct experimental evidence for the half-metallicity of various perovskite manganites. In addition, we compare these results with the first temperature-dependent tunneling spectroscopy data ever taken on a ferrimagnetic half-metal,  $\text{Fe}_3\text{O}_4$ .<sup>10-12</sup> The similarities and differences in the spectral behavior of these half-metallic ferromagnets and ferrimagnets (HMF) are discussed.

The perovskite manganites studied in this work are 200-nm-thick epitaxial films of  $\text{La}_{0.7}\text{Ca}_{0.3}\text{MnO}_3$  and  $\text{La}_{0.7}\text{Sr}_{0.3}\text{MnO}_3$  grown on single crystalline  $\text{LaAlO}_3$  substrates,<sup>13-16</sup> and 150-nm-thick  $\text{La}_{0.67}\text{Sr}_{0.33}\text{MnO}_3$  on single crystalline  $\text{SrTiO}_3$  substrates, using pulsed laser deposition.<sup>17</sup> The Curie temperatures ( $T_C$ ) for these samples are 260, 320, and 360 K, respectively. Details of the deposition procedure

and the characterizations of the structural and physical properties (including the electronic, electrical transport, magnetic, and optical properties) of the manganite epitaxial films have been reported elsewhere.<sup>13-17</sup> The  $\text{Fe}_3\text{O}_4$  sample is an epitaxial film grown on a (001)-oriented MgO substrate, also using the pulsed laser deposition technique.<sup>12</sup>

To investigate the HMF characteristics of these ferromagnetic films, we employ tunneling spectroscopy on these samples using a variable-temperature scanning tunneling microscope (STM). Tunneling spectroscopy is known to be a sensitive probe for studying the density of states of material,<sup>18</sup> particularly if the tunneling is into a many-body system characterized by a renormalized quasiparticle dispersion.<sup>19</sup> In this work, we study the tunneling spectroscopy of the magnetic epitaxial films by measuring the tunneling current as a function of the sample bias voltage. All measured spectra are highly reproducible, and the characteristics are essentially independent of the junction impedance, ranging from high impedance  $\sim 100 \text{ M}\Omega$  to low impedance  $\sim 1 \text{ M}\Omega$ . We use paramagnetic Pt for the tunneling tip to prevent possible complications in revealing the magnetic properties of the samples.

The main panels of Figs. 1(a)–1(c) illustrate the differential conductance,  $(dI/dV)/\langle I/V \rangle$ , normalized with the standard formalism given in Ref. 18, as a function of the bias voltage ( $V$ ) for  $\text{La}_{0.7}\text{Ca}_{0.3}\text{MnO}_3$  (LCMO),  $\text{La}_{0.67}\text{Sr}_{0.33}\text{MnO}_3$  (LSMO), and  $\text{Fe}_3\text{O}_4$  films at  $T=77 \text{ K}$ , respectively. The insets depict the corresponding data taken at  $T=300 \text{ K}$ . Similar measurements have also been conducted on the  $\text{La}_{0.7}\text{Sr}_{0.3}\text{MnO}_3$  sample, and the results are qualitatively similar to those obtained on the  $\text{La}_{0.67}\text{Sr}_{0.33}\text{MnO}_3$  sample, although small quantitative differences exist. These quantitative variations are given in Table I.

<sup>a)</sup>Electronic mail: jytwei@cco.caltech.edu

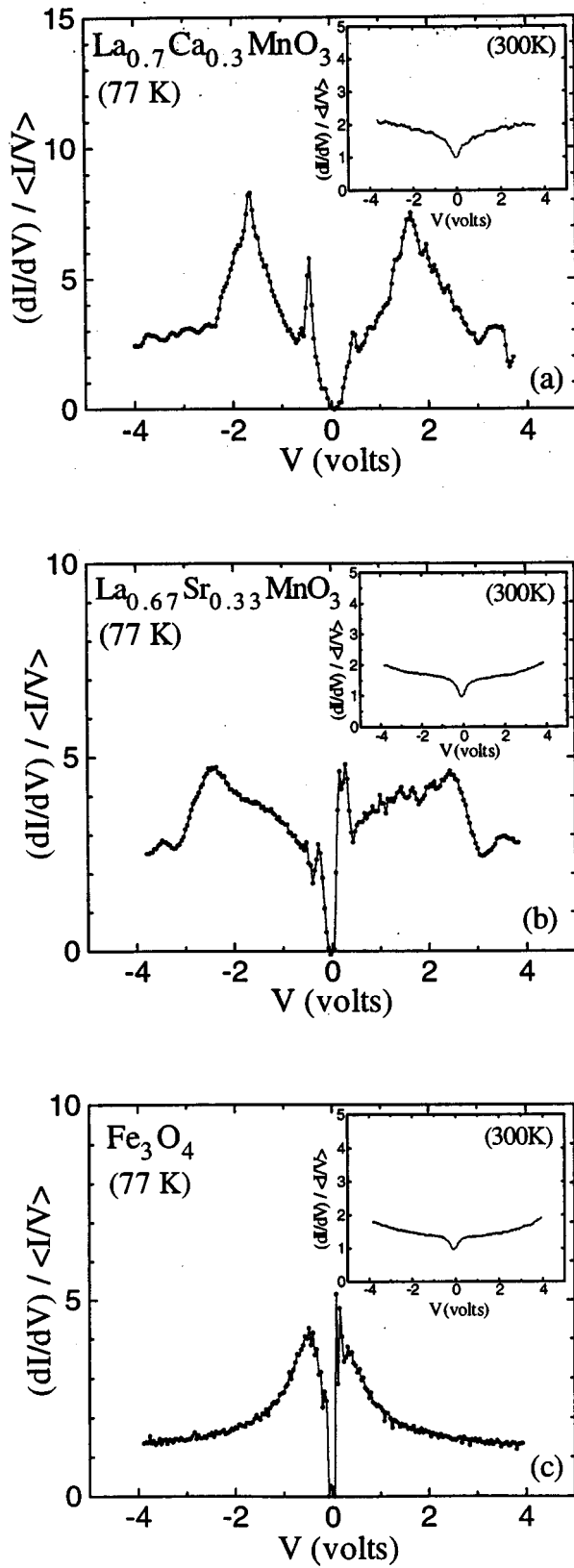


FIG. 1. The normalized differential conductance,  $(dI/dV)/\langle I/V \rangle$ , of (a)  $\text{La}_{0.7}\text{Ca}_{0.3}\text{MnO}_3$ , (b)  $\text{La}_{0.67}\text{Sr}_{0.33}\text{MnO}_3$ , and (c)  $\text{Fe}_3\text{O}_4$ , as a function of the bias voltage  $V$  at  $T=77$  K. The insets show the corresponding tunneling spectroscopy data at 300 K. The exchange energy splitting  $\Delta E_{\text{ex}}$  and the energy gap  $\Delta E_G$  values determined from the low-temperature data are given in Table I.

TABLE I. Summary of the tunneling spectroscopy measurements on the manganite and magnetite epitaxial films. The uncertainties in the energies come from spectral variations, and  $T_v$  is the Verwey temperature for  $\text{Fe}_3\text{O}_4$ .

Material	$T_C$ [K]	$\Delta E_{\text{ex}}$ [eV]	$\Delta E_G$ [eV]
$\text{La}_{0.7}\text{Ca}_{0.3}\text{MnO}_3$	260	$3.3 \pm 0.2$	$0.9 \pm 0.1$
$\text{La}_{0.7}\text{Sr}_{0.3}\text{MnO}_3$	320	$4.0 \pm 0.2$	$0.7 \pm 0.1$
$\text{La}_{0.67}\text{Sr}_{0.33}\text{MnO}_3$	360	$5.0 \pm 0.2$	$0.6 \pm 0.1$
$\text{Fe}_3\text{O}_4$	850 ( $T_v=120$ K)	$0.8 \pm 0.2$	$0.2 \pm 0.1$

Several important features of the data are noteworthy. First, two large peaks, which correspond to the density of states of the majority and minority carriers energetically separated by the on-site exchange energy, are clearly visible in each sample at 77 K. These features disappear at room temperature. Second, near zero bias voltage, the normalized differential conductivity appears to be zero for each sample at 77 K, suggesting the existence of a small energy gap  $\Delta E_G$  near the Fermi level, attributable to either a density-of-states gap in the minority band or a mobility gap in the majority band.<sup>4</sup> Furthermore,  $\Delta E_G$  is the largest in LCMO and the smallest in  $\text{Fe}_3\text{O}_4$ . Third, in the case of perovskite manganites, the exchange energy splitting  $\Delta E_{\text{ex}}$  for the same alkaline earth doping level  $x=0.3$  is larger in  $\text{La}_{0.7}\text{Sr}_{0.3}\text{MnO}_3$  ( $\Delta E_{\text{ex}} = 4.0 \pm 0.2$  eV) than in  $\text{La}_{0.7}\text{Ca}_{0.3}\text{MnO}_3$  ( $\Delta E_{\text{ex}} = 3.3 \pm 0.2$  eV), as shown in Table I. We note that the observed exchange energy in  $\text{La}_{0.7}\text{Sr}_{0.3}\text{MnO}_3$  is in good agreement with that ( $\Delta E_{\text{ex}} \approx 3.5$  eV) obtained from band-structure calculations using the local spin-density approximation.<sup>6</sup> For the Sr-doped manganites, on the other hand, the exchange energy splitting is larger in  $\text{La}_{0.67}\text{Sr}_{0.33}\text{MnO}_3$  ( $\Delta E_{\text{ex}} = 5.0 \pm 0.2$  eV) than that in  $\text{La}_{0.7}\text{Sr}_{0.3}\text{MnO}_3$ . Fourth, we note that the bandwidths of the majority and minority bands are significantly narrower in the LCMO system than those in the LSMO system. Finally, the exchange energies  $\Delta E_{\text{ex}}$  in the perovskite manganites are significantly larger than that in the magnetite  $\text{Fe}_3\text{O}_4$  ( $\Delta E_{\text{ex}} = 0.8 \pm 0.2$  eV), as summarized in Table I.

Next, we consider the physical implications of our tunneling data taken on these HMF epitaxial films. On the issue of increasing  $\Delta E_{\text{ex}}$  with the increasing alkaline doping level in the ferromagnetic state of perovskite manganites, we note that the ratio of  $\text{Mn}^{4+}$  ions ( $e_g^0 t_{2g}^3$ ) to  $\text{Mn}^{3+}$  ions ( $e_g^1 t_{2g}^3$ ) increases with increasing  $x$ , and that the crystal-field energy splitting between the  $e_g$ - and  $t_{2g}$ -orbitals results in a larger on-site exchange energy for the  $\text{Mn}^{4+}$  ions than for the  $\text{Mn}^{3+}$  ions. Hence, we would expect  $\Delta E_{\text{ex}}$  to increase with increasing  $x$ , which is also consistent with the increase of  $T_C$  observed for these two LSMO films. However, the magnitude of increase in  $\Delta E_{\text{ex}}$  with increasing  $x$  cannot be estimated easily; spin-dependent band-structure calculations will be necessary to obtain theoretical values of  $\Delta E_{\text{ex}}$  for LSMO and to compare those values with our experimental results.

Regarding the enhanced  $\Delta E_{\text{ex}}$  and reduced  $\Delta E_G$  of the Sr-doped manganites relative to the Ca-doped manganites, we note that the smaller ionic size of  $\text{Ca}^{2+}$  results in a larger degree of lattice distortion from the ideal cubic structure.<sup>20</sup> There are two important consequences of the larger degree of

lattice distortion. First, stronger electron localization occurs near the  $\text{Ca}^{2+}$  site, thereby increasing the density of localized minority carriers and reducing the density of mobile majority carriers. Hence, the conductivity of LCMO is smaller relative to that of LSMO, and the double exchange interaction between the neighboring  $\text{Mn}^{3+}$  and  $\text{Mn}^{4+}$  ions,<sup>21,22</sup> which is responsible for the ferromagnetism of these doped manganites,<sup>20–22</sup> is also weakened in the case of LCMO. Both the Curie temperature  $T_C$  and the exchange energy  $\Delta E_{\text{ex}}$  therefore decrease with the decreasing alkaline earth ion size, consistent with our experimental observation. Second, a larger deviation from the cubic structure also results in stronger hybridization of the Mn  $t_{2g}$  orbital and the oxygen  $p$  orbital. The stronger  $p-d$  hybridization is believed to enhance the half-metallicity of the manganites,<sup>4,6</sup> yielding a larger energy gap in the minority bands. This argument would be consistent with the larger  $\Delta E_G$  observed in LCMO relative to that in LSMO.

Comparing the exchange energy splitting of the perovskite manganites with that of magnetite  $\text{Fe}_3\text{O}_4$ , we note that the ferromagnetic exchange interaction for  $\text{Fe}^{2+}(e_g^2 t_{2g}^4)$  and  $\text{Fe}^{3+}(e_g^2 t_{2g}^3)$  at the  $B$  site of the spinel lattice<sup>5</sup> is compensated by the antiferromagnetic exchange interaction between the  $A$  and  $B$ -site  $\text{Fe}^{3+}$  ions.<sup>5</sup> Hence, the resulting exchange energy splitting between the minority (associated with the  $A$ -site ions) and majority (at the  $B$  site) carriers is significantly reduced, consistent with our experimental observation of a much smaller  $\Delta E_{\text{ex}}$  in  $\text{Fe}_3\text{O}_4$  than in the manganites.

The above discussion suggests that the tunneling spectra in Figs. 1(a)–1(c) can be well understood in the context of ferro- and ferrimagnetic half-metallicity. Next, we consider the temperature dependence of the tunneling spectra. In the case of  $\text{La}_{0.7}\text{Ca}_{0.3}\text{MnO}_3$ , it is easily understood that the energy splitting between the majority and minority bands disappears in the paramagnetic state at room temperature, because  $T_C \approx 260$  K. Regarding the absence of room temperature half-metallicity in  $\text{Fe}_3\text{O}_4$ , we note that magnetite  $\text{Fe}_3\text{O}_4$  is known to exhibit a sharp Verwey order-disorder transition involving  $\text{Fe}^{3+}$  and  $\text{Fe}^{2+}$  ions<sup>10</sup> below the ferrimagnetic-to-paramagnetic transition at  $T_C = 850$  K. An energy gap  $\sim 0.76$  eV in the minority bands has been predicted from the band-structure calculations.<sup>3,5</sup> However, the presence of disorder above the Verwey transition temperature  $T_V \sim 120$  K may result in smearing of the energy gap in the minority subbands, and hence the loss of half-metallic characteristics. This scenario is consistent with the NMR measurements of the longitudinal spin relaxation rate  $(1/T_1)$ ,<sup>11</sup> where anomalous temperature dependence of  $(1/T_1) \sim T^{5/2}$  for the HMF disappears and a typical metallic dependence of  $(1/T_1) \sim T$  is recovered at  $T_V < T \ll T_C$ . Recent magnetization and magnetoresistance measurements of  $\text{Fe}_3\text{O}_4$  epitaxial films also indicate the occurrence of the Verwey transition  $T_V$  at about 120 K.<sup>12</sup>

On the other hand, the disappearance of room-temperature (below  $T_C$ ) energy splitting between the majority and minority bands in both Sr-doped manganites is not easily comprehensible. This observation is nonetheless consistent with a recent finding of temperature-dependent spin-

resolved photoemission spectroscopy on  $\text{La}_{0.7}\text{Sr}_{0.3}\text{MnO}_3$ ,<sup>23</sup> where the difference between the spin density of states of the majority and minority bands decreases linearly with increasing temperature, even at temperatures well below  $T_C$ . The rapidly vanishing half-metallic ferromagnetism with increasing temperature from the surface-sensitive photoemission measurements has been attributed to the existence of surface magnetization in LSMO, which may be significantly different from the bulk magnetization. Since STM measurements are also surface sensitive, our results may also be representative of the surface magnetization, and therefore not inconsistent with the bulk half-metallic properties. This issue awaits further quantitative investigation as a function of temperature.

The research at Caltech is supported by the Packard Foundation and the National Aeronautics and Space Administration, Office of Space Science (NASA/OSS). Part of the research was performed by the Center for Space Microelectronics Technology, Jet Propulsion Laboratory, Caltech, and was sponsored by NASA/OSS.

<sup>1</sup>R. A. de Groot, F. M. Mueller, P. G. van Engen, and K. H. J. Buschow, *Phys. Rev. Lett.* **50**, 2024 (1983).

<sup>2</sup>P. G. van Engen, K. H. J. Buschow, R. Jongebreur, and M. Erman, *Appl. Phys. Lett.* **42**, 202 (1983).

<sup>3</sup>R. A. de Groot and K. H. J. Buschow, *J. Magn. Magn. Mater.* **54–57**, 1377 (1986).

<sup>4</sup>V. Yu. Irkhin and M. I. Katsnel'son, *Phys. Usp.* **37**, 659 (1994).

<sup>5</sup>A. Yanase and K. Siratori, *J. Phys. Soc. Jpn.* **53**, 312 (1984).

<sup>6</sup>W. E. Pickett and D. J. Singh, *Phys. Rev. B* **53**, 1146 (1996).

<sup>7</sup>F. Heusler, *Verh. Dtsch. Phys. Ges.* **5**, 219 (1903).

<sup>8</sup>H. Y. Hwang, S.-W. Cheong, N. P. Ong, and B. Batlogg, *Phys. Rev. Lett.* **77**, 2041 (1996).

<sup>9</sup>J. Z. Sun, W. J. Gallagher, P. R. Duncombe, L. Krusin-Elbaum, and R. A. Altman, *Appl. Phys. Lett.* **69**, 3266 (1996).

<sup>10</sup>E. J. Verwey, P. W. Haayman, and F. C. Romeijn, *J. Chem. Phys.* **15**, 458 (1947).

<sup>11</sup>T. Mizoguchi and M. Inoue, *J. Phys. Soc. Jpn.* **21**, 310 (1966).

<sup>12</sup>G. Q. Gong, A. Gupta, G. Xiao, W. Qian, and V. P. Dravid, *Phys. Rev. B* **56**, 5096 (1997).

<sup>13</sup>N.-C. Yeh, R. P. Vasquez, D. A. Beam, C. C. Fu, J. Huynh, and G. Beach, *J. Phys.: Condens. Matter* **9**, 3713 (1997); N.-C. Yeh *et al.*, *J. Appl. Phys.* **81**, 5499 (1997); *Mater. Res. Soc. Symp. Proc.* **474**, 145 (1997).

<sup>14</sup>J. Y. T. Wei, N.-C. Yeh, and R. P. Vasquez, *Phys. Rev. Lett.* **79**, 5150 (1998).

<sup>15</sup>R. P. Vasquez, *Phys. Rev. B* **54**, 14 938 (1996).

<sup>16</sup>A. V. Boris, N. N. Kovaleva, A. V. Bazhenov, A. V. Samoilov, N.-C. Yeh, and R. P. Vasquez, *J. Appl. Phys.* **81**, 5756 (1997).

<sup>17</sup>A. Gupta, G. Q. Gong, G. Xiao, P. R. Duncombe, P. Lecoeur, P. Trouilloud, Y. Y. Wang, V. P. Dravid, and J. Z. Sun, *Phys. Rev. B* **54**, R15 629 (1997); *Appl. Phys. Lett.* **67**, 3494 (1995).

<sup>18</sup>For a review, see, for example, R. M. Feenstra, *Surf. Sci.* **299/300**, 965 (1994); R. J. Hamers, *Annu. Rev. Phys. Chem.* **40**, 531 (1989).

<sup>19</sup>G. D. Mahan, *Many Particle Physics* (Plenum, New York, 1990); E. L. Wolf, *Principles of Electron Tunnel Spectroscopy* (Oxford University Press, Oxford, 1985).

<sup>20</sup>J. B. Goodenough, A. Wold, R. J. Arnott, and N. Menyuk, *Phys. Rev.* **124**, 373 (1961); J. B. Goodenough, *Progress in Solid State Chemistry*, Vol. 5, edited by H. Reiss (Pergamon, Oxford, 1971).

<sup>21</sup>G. H. Jonker and J. H. van Santen, *Physica* **16**, 337 (1950); J. H. van Santen and G. H. Jonker, *ibid.* **16**, 599 (1950).

<sup>22</sup>C. Zener, *Phys. Rev.* **82**, 403 (1951); E. O. Wollan and W. C. Koehler, *ibid.* **100**, 545 (1955).

<sup>23</sup>J. H. Park, E. Vescovo, H.-J. Kim, C. Kwon, R. Ramesh, and T. Venkatesan, *Nature* (London) (in press); *Phys. Rev. Lett.* (submitted).